

**Diagnostic and prognostic value of ECG-predicted hypertension-mediated  
left ventricular hypertrophy using machine learning**

Hafiz Naderi<sup>1,2,3</sup>, Julia Ramírez<sup>1,4,5</sup>, Stefan van Duijvenboden<sup>1,6</sup>, Esmeralda Ruiz Pujadas<sup>7</sup>, Nay Aung<sup>1,2,3</sup>, Lin Wang<sup>8</sup>, Bishwas Chamling<sup>9,10,11</sup>, Marcus Dörr<sup>9,10</sup>, Marcello R P Markus<sup>9,10,11</sup>, C. Anwar A Chahal<sup>1,2,12,13</sup>, Karim Lekadir<sup>7,14</sup>, Steffen E Petersen\*<sup>1,2,3,15</sup>, Patricia B Munroe\*<sup>1,3</sup>

1. William Harvey Research Institute, Queen Mary University of London, Charterhouse Square, London, UK
2. Barts Heart Centre, St Bartholomew's Hospital, Barts Health NHS Trust, West Smithfield, London, UK
3. National Institute of Health and Care Research Barts Biomedical Research Centre, Queen Mary University of London, Charterhouse Square, London, UK
4. Aragon Institute of Engineering Research, University of Zaragoza, Spain, CIBER-BBN, Spain
5. Centro de Investigación Biomédica en Red - Biomateriales, Bioingeniería y Nanomedicina, University of Zaragoza, Spain
6. Big Data Institute, La Ka Shing Centre for Health Information and Discovery, University of Oxford, UK
7. Faculty of Mathematics and Computer Science, University of Barcelona, Spain
8. School of Electronic Engineering and Computer Science, Queen Mary University of London, UK
9. Department of Internal Medicine B, University Medicine Greifswald, Germany
10. German Center for Cardiovascular Research (DZHK), partner site Greifswald, Germany
11. German Center for Diabetes Research (DZD) partner site Greifswald, Germany
12. Center for Inherited Cardiovascular Diseases, WellSpan Health, Lancaster, PA, USA
13. Department of Cardiovascular Diseases, Mayo Clinic, Rochester, MN, USA
14. Institució Catalana de Recerca i Estudis Avançats (ICREA), Barcelona, Spain
15. Health Data Research UK, London, UK

\*SEP and PBM jointly supervised the work.

SEP ([s.e.petersen@qmul.ac.uk](mailto:s.e.petersen@qmul.ac.uk)) and PBM ([p.b.munroe@qmul.ac.uk](mailto:p.b.munroe@qmul.ac.uk)) are the corresponding authors.

Word count: 6,360

## **Abstract**

### **Background**

Four hypertension-mediated left ventricular hypertrophy (LVH) phenotypes have been reported using cardiac magnetic resonance (CMR): normal LV, LV remodeling, eccentric and concentric LVH, with varying prognostic implications. The electrocardiogram (ECG) is routinely used to detect LVH, however its capacity to differentiate between LVH phenotypes is unknown. This study aimed to classify hypertension-mediated LVH from the ECG using machine learning (ML) and test for associations of ECG-predicted phenotypes with incident cardiovascular outcomes.

### **Methods**

ECG biomarkers were extracted from the 12-lead ECG of 20,439 hypertensives in UK Biobank (UKB). Classification models integrating ECG and clinical variables were built using logistic regression, support vector machine (SVM) and random forest. The models were trained in 80% of the participants, and the remaining 20% formed the test set. External validation was sought in 877 hypertensives from the Study of Health in Pomerania (SHIP). In the UKB test set, we tested for associations between ECG-predicted LVH phenotypes and incident major adverse cardiovascular events (MACE) and heart failure.

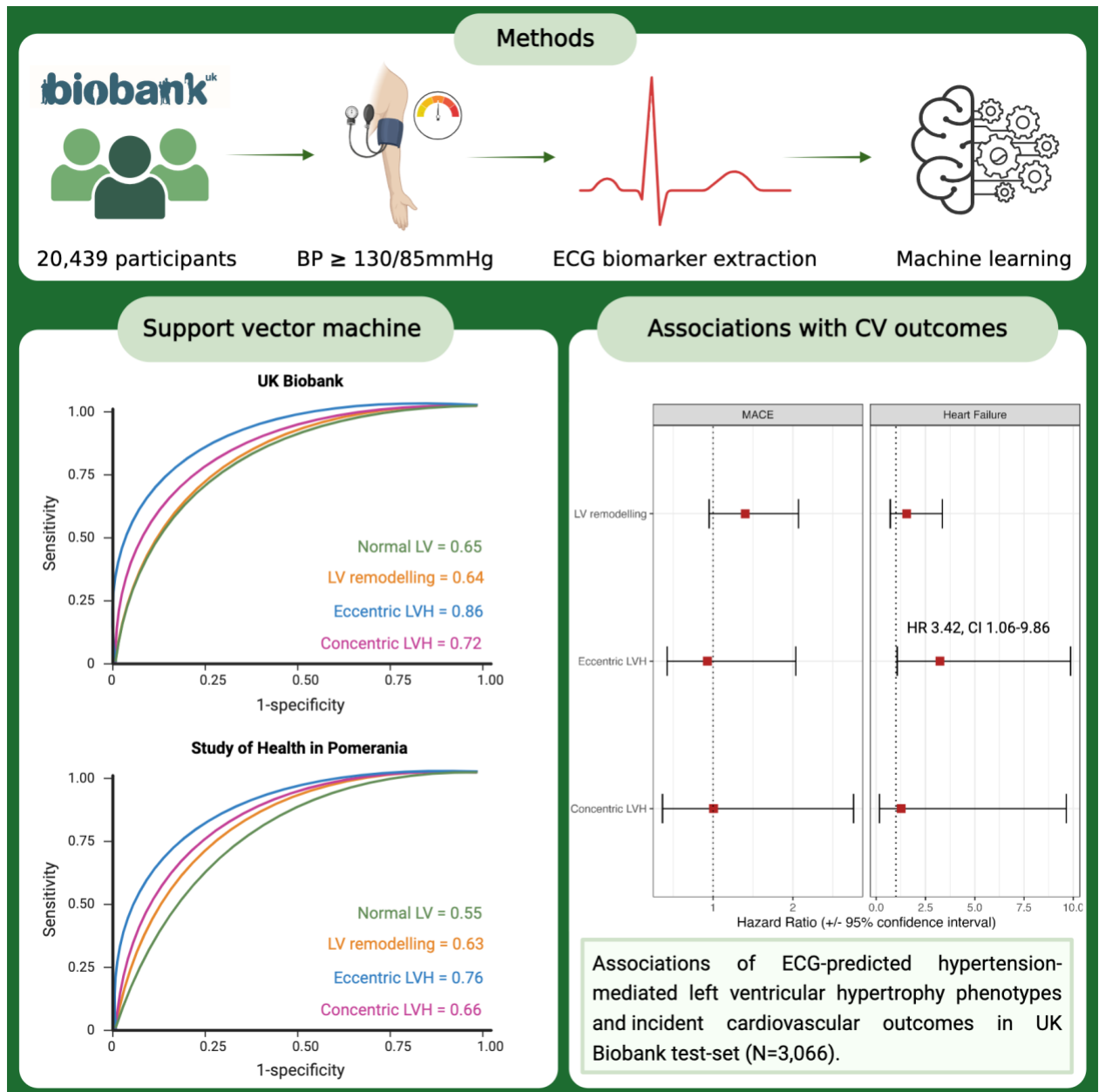
### **Results**

Among UKB participants 19,408 had normal LV, 758 LV remodeling, 181 eccentric and 92 concentric LVH. Classification performance of the three models was comparable, with SVM having a slightly superior performance (accuracy 0.79, sensitivity 0.59, specificity 0.87, AUC 0.69) and similar results observed in SHIP. There was superior prediction of eccentric LVH in both cohorts. In the UKB test set, ECG-predicted eccentric LVH was associated with heart failure (HR 3.42, CI 1.06-9.86).

### **Conclusions**

ECG-based ML classifiers represent a potentially accessible screening strategy for the early detection of hypertension-mediated LVH phenotypes.

# Graphical abstract



## Non-standard Abbreviations and Acronyms

AI	Artificial intelligence
AUC	Area under the curve
BP	Blood pressure
CHD	Coronary heart disease
CI	Confidence interval
CMR	Cardiac magnetic resonance imaging
CV	Cardiovascular
CVD	Cardiovascular disease
DBP	Diastolic blood pressure
ECG	Electrocardiogram
HCM	Hypertrophic cardiomyopathy
LR	Logistic Regression
LV	Left ventricle
LVH	Left ventricular hypertrophy
MICE	Multivariate Imputation by Chained Equations
ML	Machine learning
mmHg	Millimetre of mercury
MRI	Magnetic resonance imaging
P	P-value
RF	Random forest
ROC	Receiver operator curves
SBP	Systolic blood pressure
SHIP	Study of Health in Pomerania
SVM	Support vector machine
UKB	UK Biobank

## **Introduction**

Hypertension is the most common cause of left ventricular hypertrophy (LVH), and both are strong predictors of cardiovascular (CV) morbidity and mortality.<sup>1,2</sup> The diagnosis of hypertension-mediated LVH has relied on cardiac imaging, such as echocardiography and cardiac magnetic resonance (CMR).<sup>3,4</sup> Using CMR imaging, four distinct hypertension-mediated LVH phenotypes have been reported: normal left ventricle (LV), LV remodeling, eccentric LVH and concentric LVH.<sup>5</sup> The spectrum of LVH phenotypes has been shown to have varying prognostic implications, with worse CV outcomes reported in eccentric and concentric LVH.<sup>6,7</sup> Due to the global burden of hypertension, a cost-effective approach in detecting LVH phenotypes is required to meet clinical demand. Before the advent of CV imaging, the electrocardiogram (ECG) had been used clinically to screen for LVH in hypertension.<sup>8-10</sup> However, its capacity to detect the four CMR-defined LVH phenotypes is unknown.

Hypertension clinical guidelines endorse using the 12-lead ECG in individuals to screen for LVH.<sup>3,4,11</sup> The ECG is a readily available and low-cost first line diagnostic tool performed on most patients during an acute care visit and follow-up of chronic CV conditions. In recent years, the transition to digitised ECG in electronic healthcare records has paved opportunities for ECG-based diagnostic and prognostic predictions. Moreover, the use of wearable technology and smartphones have increased its accessibility. Early detection of hypertension-mediated LVH can enable regular healthcare follow-up, rigorous CV risk management and timely initiation of effective blood pressure (BP)-reducing therapies. However, accurate reporting of the ECG is challenging for clinicians, and any improvement in automated analysis could ensure timely diagnosis and treatment of hypertensive patients with LVH.<sup>12-14</sup> A machine learning (ML) tool to detect hypertension-mediated LVH phenotypes could reduce the number of unnecessary CMR scans, allowing them to be used more efficiently, thus reducing waiting times. This is also of clinical significance as the ECG features derived from classifying hypertension-mediated LVH phenotypes may be used as surrogate markers to predict clinical outcomes in hypertensives.

This study uses ML techniques to explore the diagnostic and prognostic value of ECG-predicted hypertension-mediated LVH phenotypes. We hypothesized that a selection of ECG biomarkers and

clinical variables could classify hypertension-mediated LVH phenotypes defined by CMR imaging and that these ECG-predicted LVH phenotypes would be associated with incident CV outcomes.

## Methods

### UK Biobank sample selection

The UK Biobank (UKB) is a large prospective population study where demographics, medication history, electronic health records, biomarkers and genomics were collected in half a million participants aged 40-69 years when recruited between 2006 and 2010 from across the United Kingdom. The UKB imaging study was launched in 2015 with the aim of scanning 20% of the original cohort, that is 100,000 participants.<sup>15</sup> The details of the UKB CMR protocol have been described elsewhere.<sup>16</sup>

A total of 44,817 participants had completed the UKB imaging study at the time of analysis. Of these, 37,651 participants had both ECG and CMR data available. Hypertensive participants (N=23,042) were identified according to the ‘high normal’ BP grade of  $\geq 130/85$ mmHg based on the 2018 European Society of Cardiology/European Society of Hypertension (ESC/ESH) guideline.<sup>3</sup> In UKB, BP readings from the imaging visit were analyzed as these were taken on the same day as the CMR study and 12-lead resting ECG. Each participant had two manual BP readings using a validated automated BP monitor or a manual sphygmomanometer. After calculating the average BP values, we adjusted for medication use by adding 15 and 10 mmHg to SBP and DBP, respectively, for participants reported to be taking BP-lowering medication.<sup>17</sup> We further defined hypertension by selecting relevant data fields from the UKB data showcase, including hypertension self-reported by participants, formal diagnosis from primary care physician and BP medication use. Participants with other causes of LVH (N=2,603) were excluded by reviewing exome sequence data for genes implicated in hypertrophic cardiomyopathy.<sup>18</sup> The remaining hypertensive participants (N=20,439) were categorized into the four hypertension-mediated LVH phenotypes using a mass-to-volume ratio. Indexing for body surface area was performed using the Mosteller formula.<sup>19</sup> The data fields selected from UKB are shown in Supplementary Table 1. Figure 1 illustrates the UKB sample selection process.

### **ECG biomarker extraction**

Full 15-second 12-lead ECG signals of each of the 20,739 participants were analyzed semi-automatically using a custom algorithm written in MATLAB (version 2021a, Mathworks Inc.) to derive 23 biomarkers (Supplementary Table 2) with a known physiological association with LVH.<sup>20</sup> Only the independent ECG leads (I, II, V1-6) were analyzed. Butterworth filter (1-45Hz) was applied to attenuate baseline wander and high-frequency noise. ECG biomarkers from each independent lead were treated as individual features. In addition, global ECG features were calculated as the median value across the independent leads. The applied algorithm for extracting ECG biomarkers is detailed elsewhere.<sup>21</sup>

### **Ascertainment of clinical variables**

In addition to ECG biomarkers, we also included clinical variables known to be associated with LVH (**Table 1**) in the classification model. Each clinical variable was defined by either a self-reported questionnaire or biochemistry results. Participants with serum total cholesterol of  $\geq 5$ mmol/L and Hemoglobin A1c (HbA1c)  $\geq 48$  mmol/mol at the baseline visit were considered to have hypercholesterolemia and diabetes mellitus, respectively. We corrected total and non-HDL cholesterol values for participants on cholesterol-lowering medication by dividing the total cholesterol by 0.73 and non-HDL cholesterol by 0.66.<sup>22</sup> The presence of tobacco use was ascertained using self-reported questionnaires, with smoking status classified categorically as current, previous or never. Alcohol consumption was classified as current or never.

### **Supervised machine learning techniques**

Three supervised ML algorithms were evaluated for classification: logistic regression, support vector machine (SVM) and random forest (RF). The algorithms were implemented in MATLAB, and the fit multiclass models for SVMs or other classifiers (fitcecoc) function was used to build the logistic regression and SVM classifiers.<sup>23</sup> The fit ensemble of learners for classification (fitcensemble) was used to build the RF classifier.<sup>24</sup> In our experiments, the dataset was split into a training set (80%) for learning and a test set (20%) for performance evaluation. We applied 10-fold cross-validation to the training set. The metrics we used to assess classifier performance in the test set included: accuracy, sensitivity,

specificity, precision, F1 score and area under the receiver operator curve (AUC). Further details of the models are described previously.<sup>21</sup>

### **External validation in Study of Health in Pomerania**

The Study of Health in Pomerania (SHIP) is a population-based study investigating common risk factors and subclinical diseases from a random cluster sample drawn from the population of West Pomerania in Northeast of Germany.<sup>25,26</sup> SHIP consists of two independent cohorts: SHIP-START (recruited between 1997 to 2001) and SHIP-TREND (recruited between 2008 to 2012). Study participants for both cohorts were sampled from the general adult population aged 20-79 in West Pomerania. This study used the second follow-up of SHIP-START (SHIP-START-2) and baseline SHIP-TREND-0 as these were the studies with both 12-lead ECG and CMR data. The populations comprised 2,333 participants for SHIP-START-2 and 4,420 participants for SHIP-TREND-0.<sup>26</sup> A total of 1,474 participants from SHIP had both CMR and ECG data. The same definition of hypertension was applied based on BP readings, medication use and diagnosis, yielding a total of 877 hypertensives in SHIP. The same ECG biomarkers and clinical features as per UKB analysis were extracted. For classification, the whole SHIP cohort was treated as a test set. Therefore, down-sampling was not applied. The best-performing ML model (SVM) was taken forward for external validation in SHIP.

### **Associations with cardiovascular outcomes in UK Biobank**

Longitudinal data on clinical outcomes of UKB participants is recorded using linkage to Hospital Episode Statistics (HES) and the UK death register.<sup>27</sup> All UKB participants consented to be followed up. In this study, the primary endpoint was major adverse cardiovascular events (MACE), defined as either hospitalization or death due to fatal/non-fatal myocardial infarction, stroke or ventricular arrhythmias. Cases were identified using relevant International Classification of Disease, 9<sup>th</sup> or 10<sup>th</sup> Revision (ICD-9, ICD-10), or Office of Population Censuses and Surveys version 4 (OPCS 4) Classification of Interventions and Procedures codes in the health-related records or death register (Supplementary Table 3). An additional analysis was performed testing for association with heart failure separately. These clinical outcomes were selected due to their association with hypertension

from the literature and clinical expertise. The follow-up period was determined by the first appearance of ICD-9, ICD-10 or OPSC4 codes in either health record or death register data since the UKB imaging visit. Participants with prevalent events at the time of UKB enrolment were excluded from the survival analyses. Participants who did not experience an event were censored at death or the end of the follow-up period (30 November 2022).

### **Statistical analyses**

Statistical analyses were performed using R version 4.0.3 and RStudio Version 1.3.1093.<sup>28</sup> After excluding missing or extreme ECG values (outside the range defined by the quartiles  $\pm 1.5 \times$  interquartile range) the Classification And REgression Training (CARET) package in R was used for correlation analysis, and highly correlated ECG biomarkers were omitted (correlation coefficient threshold of  $\pm 0.9$ ).<sup>29</sup> ECG biomarkers with less than 10% of missing data were imputed using the Multivariate Imputation by Chained Equations (MICE) package in R.<sup>30</sup> In order to address the imbalance in the dataset, down-sampling was applied using the CARET package in the training set to match the proportion of participants in the minority LVH group. A chi-squared test was used to rank the features in terms of feature importance score.

Descriptive statistics are presented as median (interquartile range) for continuous variables or frequency (percentage) for categorical variables. The distribution of continuous data was assessed by visual inspection of the histograms and confirmed by the Shapiro-Wilk test. Baseline clinical and ECG characteristics of the hypertension-mediated LVH phenotypes were statistically compared with the normal LV group. To assess for associations, the ANOVA test was used for continuous data and the chi-squared test for categorical data. For all analyses, a two-tailed p-value  $<0.05$  was deemed statistically significant.

Associations between the ECG-predicted phenotypes and clinical outcomes were performed in the UKB test set (N = 3,066) using multivariable-adjusted Cox proportional hazard regression, setting normal LV as the reference group. For each clinical outcome the model was adjusted for age, sex and body

mass index. Hazard ratios (HR) were reported with 95% confidence intervals (CI) to derive risk for each LVH phenotype compared to the normal LV group.

## Results

### Study population

The clinical and ECG characteristics of the UKB participants stratified by hypertension-mediated LVH phenotypes are presented in Table 1. Among the 20,439 hypertensive participants in UKB, 19,408 (95.0%) had normal LV, 758 (3.7%) had LV remodeling, 181 (0.9%) eccentric LVH and 92 (0.5%) concentric LVH. Overall, the cohort had an average age of 66 years, and 46% were female. In the total hypertensive cohort, the frequency of participants with LVH criteria for Sokolow-Lyon and Cornell voltage on the ECG was 2% and 8%, respectively.

Table 2 shows the baseline characteristics of the SHIP validation cohort. In SHIP there were 877 participants with hypertension, of which 704 (80.3%) had normal LV, 134 (15.3%) LV remodeling, 12 (1.4%) participants with eccentric LVH and 27 (3.1%) with concentric LVH. The average age was 56 years, and 39% were female. Overall, the frequency of participants with LVH criteria for Sokolow-Lyon and Cornell voltage on the ECG was 6% and 9%, respectively.

### Machine learning model performance in UK Biobank

Supplementary Figure 1 shows the ranking of the top 40 features across all ML models using chi-squared feature selection. The top clinical features were sex and age, and the highest-ranking ECG predictors of LVH were ventricular rate and QRS amplitude in V4.

The performance metrics of the supervised ML classifiers (logistic regression, SVM and RF) using both ECG and clinical variables in UKB are shown in Table 3. Classification with each method was comparable in the test set, with SVM showing the most consistent performance with 0.79 accuracy, 0.59 sensitivity, 0.87 specificity, 0.78 precision, 0.67 F1 score and AUC 0.69. Using SVM, the classification of eccentric LVH (AUC 0.86) and concentric LVH (0.72) was superior to normal LV (0.65) and LV remodeling (0.64) phenotypes, as shown in Figure 2. The ECG biomarkers enhanced the

model performance of the SVM classifier in UKB, compared to clinical variables alone (AUC values of 0.69 and 0.58, respectively), as illustrated in Figure 2.

### **External validation in Study of Health in Pomerania**

External validation in the SHIP cohort using SVM showed a similar performance to UKB with 0.75 accuracy, 0.51 sensitivity, 0.85 specificity, 0.63 precision, 0.56 F1 score and 0.65 AUC (Table 3). Akin to UKB, the classification of eccentric LVH (AUC 0.76) and concentric LVH (0.66) was superior to normal LV (0.55) and LV remodeling (0.63) phenotypes. The ECG biomarkers also enhanced the model performance of the SVM classifier in the SHIP cohort, compared to clinical variables alone (AUC values of 0.65 and 0.61, respectively, shown in Figure 2).

### **Association of ECG-predicted LVH phenotypes with CV outcomes**

Figure 3 shows the associations between ECG-predicted hypertension-mediated LVH phenotype using SVM and the clinical outcomes MACE and heart failure in the UKB test set (N = 3,066). There was no statistically significant association with MACE (Supplemental Table 4), however the hazard ratio of heart failure was 3.2 times higher (HR 3.24, CI: 1.06-9.86) in hypertensives with eccentric LVH with normal LV set as the reference group (Supplementary Table 4).

## Discussion

In UKB, a combination of ECG biomarkers and clinical variables was able to discriminate between hypertension-mediated LVH phenotypes using supervised ML techniques. The ML classifiers had similar performances, with slight superiority using SVM. External validation in the SHIP cohort using SVM demonstrated the robustness of the model with reproducible results. We observed incremental value in using the 12-lead ECG compared to clinical variables alone for hypertension-mediated LVH detection. The classification of eccentric LVH and concentric LVH was superior to normal LV and LV remodeling phenotypes in both UKB and the SHIP cohort. Furthermore, we observed a strong association between the ECG-predicted eccentric LVH group in the UKB test set and heart failure (HR 3.24, CI: 1.06-9.86), indicating there is potential clinical relevance of the model.

This is the first ML study to classify hypertension-mediated LVH phenotypes from the ECG. Ventricular rate and QRS amplitude in the precordial leads were the most influential ECG features in the model. The other top ECG predictors of LVH were measurements relating to the QRS complex, such as QRS duration, QRS descending slope and Sokolow-Lyon criteria, which are derived from amplitude measures of the QRS complex. Change in the QRS complex is a marker of electrical remodeling seen in LVH, which has been postulated to be due to the increase in the muscle mass of the LV mounting the forces of the LV potential. However, the increased QRS voltage is seen only in a minority of LVH cases in both clinical and animal studies, and consequently, voltage criteria suffer from a high number of false negative results and low sensitivity.<sup>31</sup> In prior work, ECG predictors of LVH have suffered low sensitivity, ranging from 15-30%.<sup>32</sup> Using a combination of ECG and clinical variables, our sensitivity values were higher, with over 50% using SVM, without compromising specificity (87% using SVM).

The results across all models were comparable, with SVM demonstrating the best overall model performance in classifying hypertension-mediated LVH phenotypes. There is no direct comparative study; however, Beneyto and colleagues (2023) also found SVM to be superior in detecting

hypertension as the cause of LVH, compared to the decision tree and RF models.<sup>33</sup> The authors defined LVH as maximal LV wall thickness greater than 12mm in diastole and found that SVM had the optimal balance between specificity of 86% and sensitivity of 31%. Beneyto *et al* used a combination of clinical, laboratory and ECG features in their models. They identified systolic BP and the number of anti-hypertensive medications among the most significant features for classification. However, as ECG features were not included, this precludes direct comparison with our study.

We validated our findings in an independent cohort, and the results demonstrated robustness of the ML model. Although both cohorts were European, they had differing clinical profiles. Compared to UKB, the SHIP cohort was younger (66 years vs 56 years) and had a higher incidence of hypercholesterolemia (19% vs 79%). The SHIP cohort is noted to be a ‘high-risk’ population compared to the relatively ‘healthy’ cohort of UKB. Despite the differing risk profiles of these cohorts, our model’s comparative performance indicated potential translatability to community populations but also the requirement for further validation experiments.

We speculate that the superior prediction of concentric LVH and eccentric LVH is perhaps due to the distinct geometry of these phenotypes on imaging. A dilated LV characterises eccentric LVH, while concentric LVH is synonymous with a thickened LV wall and small LV cavity size. In contrast, normal LV and LV remodeling are less distinct, hence the inferior classification of these phenotypes using ML.

Following the validation of the model in the SHIP dataset, we were interested in assessing whether the ECG-predicted phenotypes were associated with clinical outcomes. Using the test set in UKB (N=3,066) we observed a significant association between eccentric LVH and heart failure with a 3.2 increased hazard rate of heart failure compared to those with normal LV geometry. Hypertension leads to heart failure through LVH and LV diastolic dysfunction, eventually progressing to LV systolic impairment in a subset of patients in the presence of chronic volume and pressure overload.<sup>34,35</sup> The lack of association with outcomes in the other LVH phenotypes is likely due to the relatively short follow-up period in UKB and relatively small population size of the test set. However, with the UKB

aiming to scan 100,000 participants, there is potential to review outcomes in the future with greater numbers.

Nauta *et al* (2020) showed that patients with heart failure with eccentric LVH have a clinical and biomarker phenotype that is distinctly different from those with concentric LVH.<sup>36</sup> In a retrospective post-hoc analysis of 1,015 patients with heart failure (LV ejection fraction <40%), the majority of patients (N=873) had eccentric LVH and were, on average, younger (P=0.005) and had a lower ejection fraction (P<0.001). The authors also found that beta-blocker up-titration was associated with a mortality benefit in heart failure with eccentric but not concentric LVH (P<0.001). Hypertension is an important risk factor for heart failure, therefore, improvements in screening are essential to reduce its burden and associated morbidity.<sup>37</sup>

Although the results are promising, further development and testing are required before implementation. For clinical applicability, the ML methods would need to be integrated into a point-of-care application or directly into ECG machines. Developing a model for single lead ECG would also be of interest, particularly in the era of wearable and smartphone technology. Considering the high global burden of hypertension, a cost-effective and accurate risk prediction of LVH may facilitate population screening and timely treatment in individuals with subclinical disease and could serve as surrogate markers for predicting outcomes. We have shown that eccentric LVH classified by ML is strongly associated with heart failure. This provides an opportunity to enhance targeted and personalized therapy for improvement in clinical outcomes of heart failure.

.The rate of new blood pressure-lowering therapies reaching the market has substantially declined, in part due to a lack of new targets for investigation. There is current interest in exploring the anti-fibrotic potential of sacubitril/valsartan (an angiotensin receptor-neprilysin inhibitor) in a clinical population, guided by imaging. REVERSE-LVH is a prospective, randomised, blinded endpoint (PROBE) clinical trial, designed to compare the effects of 52 weeks of treatment with sacubitril/valsartan with valsartan (an angiotensin receptor inhibitor) on the primary endpoint of change in interstitial volume measured

by CMR in patients with hypertension and LVH.<sup>38</sup> The UKB repeat imaging study may be an avenue to explore ECG-based classifiers in the reversal of LVH in hypertension.

Over thirty percent of adults worldwide have hypertension. Therefore, the potential cost-benefit of early detection of hypertension-mediated LVH is immense. Hypertension guidelines recommend the 12-lead ECG is performed in all patients newly diagnosed with hypertension.<sup>39</sup> This provides an opportunity to compare the cost-benefit of ECG-based ML classification of LVH to that of conventional management. Important challenges will be to compare different sensitivity and specificity thresholds for the model to balance the trade-off between diagnostic accuracy and the economic benefit of downstream testing with potential false positive results. In order to implement an ECG-based ML screening strategy for LVH, it will be important to evaluate the cost-effectiveness under various clinical and cost scenarios.

Although we were able to perform external validation, an important limitation is that both cohorts are predominantly White European ancestry, therefore, further work is warranted to elucidate the classification of hypertension-mediated LVH in other ethnicities. Furthermore, our experiments included only ECG and clinical characteristics as features in the ML models. The rationale for this was to incorporate features that are accessible in a wide range of healthcare settings. Nevertheless, there is potential to include additional features to improve model performance and further personalize the ML algorithm. The UKB has access to numerous biomarkers and healthcare data such as BP medication history, biochemistry results, metabolomics, and genetic data, including genetic risk scores. These data could be incorporated into models for further development. In this study, we used three supervised ML approaches, and these models can be developed further to increase accuracy. Models using XGBoost (Extreme Gradient Boosting), decision trees and K-nearest neighbor are attractive options.<sup>40-42</sup> Agnostic approaches such as unsupervised ML and deep learning (DL) may also be used, and these may identify novel signals in the ECG associated with LVH.

## **Perspectives**

This study demonstrates the potential of ECG-predicted ML classifiers to detect hypertension-mediated LVH phenotypes. A ML tool to detect hypertension-mediated LVH phenotypes may enhance clinician ECG interpretation and expedite workflow by ensuring that advanced imaging tests are used for those who need it most, thereby reducing unnecessary testing and subsequent waiting times. ML models based on ECG predictors offer new opportunities for improved and potentially cost-effective LVH detection, enhancing the capabilities of non-specialists. Future work will require validation testing in ethnically diverse cohorts with efforts to continue to improve performance metrics using auxiliary tools and health economics studies to assess the cost-benefit of this approach.

### **Conclusions**

ECG-based classifiers could discriminate between the four hypertension-mediated LVH phenotypes with external validation demonstrating robustness. We also observed a strong association between the ECG-predicted eccentric LVH and heart failure indicating there is important prognostic information gained from the model. This automated approach enhances the capabilities of non-specialists and potentially represents an accessible screening strategy for the early detection of hypertensives with LVH.

## **Novelty and Relevance**

### **What is new?**

- Supervised ML techniques using ECG and clinical data can detect LVH and discriminate between hypertension-mediated LVH phenotypes.
- The ECG provides important prognostic information and may provide clinicians with valuable information to assess CVD risk in hypertensives, particularly in low-resource settings.
- This automated approach may represent an efficient and accessible screening strategy for detecting subclinical LVH in hypertensives.

### **What is relevant?**

- Hypertension clinical guidelines endorse using the 12-lead ECG in hypertensives to screen for LVH.
- The diagnosis of hypertension-mediated LVH has relied on cardiac imaging, such as echocardiography and CMR.
- The potential cost implications of deploying and interpreting these imaging modalities as a screening strategy to detect hypertension-mediated LVH is not economically feasible.

### **Clinical/Pathophysiological implications?**

The ECG is a ubiquitous and low-cost diagnostic tool. In recent years, the transition to digitized ECG in electronic healthcare records and wearable technology has paved opportunities for ECG-based diagnostic and prognostic predictions. Early detection of hypertension-mediated LVH can enable regular healthcare follow-up, rigorous CV risk management and timely initiation of effective BP-reducing therapies.

### **Ethics statement**

This study complies with the Declaration of Helsinki; the work was covered by the ethical approval for UK Biobank studies from the NHS National Research Ethics Service on 17th June 2011 (Ref 11/NW/0382) and extended on 18 June 2021 (Ref 21/NW/0157) with written informed consent obtained from all participants. The work related to Study of Health in Pomerania is via application reference number SHIP/2023/31/D. The study is covered by the overall ethical approval for SHIP studies approved by the Ethics Committee at the University Medicine Greifswald, Germany.

### **Data Availability Statement**

The data underlying this article were provided by the UK Biobank under access application 2964. UK Biobank will make the data available to bona fide researchers for all types of health-related research that is in the public interest, without preferential or exclusive access for any persons. All researchers will be subject to the same application process and approval criteria as specified by UK Biobank. For more details on the access procedure, see the UK Biobank website: <http://www.ukbiobank.ac.uk/register-apply/>.

### **Acknowledgements**

This study was conducted using the UK Biobank resource under access application 2964. We would like to thank all the participants, staff involved with planning, collection and analysis, including core lab analysis of the CMR imaging data. Graphical abstract was created using Biorender.com.

### **Sources of funding**

HN was supported by the British Heart Foundation Pat Merriman Clinical Research Training Fellowship (FS/20/22/34640). JR acknowledges fellowship RYC2021-031413-I from the European Union “NextGenerationEU/PRTR” and MCIN/AEI/10.13039/501100011033. NA acknowledges support from Medical Research Council for his Clinician Scientist Fellowship (MR/X020924/1). SEP acknowledges the British Heart Foundation for funding the manual analysis to create a cardiovascular magnetic resonance imaging reference standard for the UK Biobank imaging resource in 5000 CMR

scans ([www.bhf.org.uk;PG/14/89/31194](http://www.bhf.org.uk;PG/14/89/31194)). SEP and PBM acknowledge support from the National Institute for Health and Care Research (NIHR) Biomedical Research Centre at Barts (NIHR202330). SEP, KL and ER have received funding from the European Union's Horizon 2020 research and innovation programme under grant agreement No 825903 (euCanSHare project). KL has received funding from the European Union's Horizon 2020 research and innovation programme under grant agreements No 101080430 (AI4HF project) and No. 101057849 (DataTools4Heart project). The Study of Health in Pomerania (SHIP) is part of the Community Medicine Research net (CMR) (<http://www.medizin.uni-greifswald.de/icm>) of the University Medicine Greifswald, which is supported by the German Federal Ministry of Education and Research (BMBF, grant number: 01ZZ96030 and 01ZZ0701) and the Federal State of Mecklenburg-West Pomerania. MRI scans in SHIP-2 and SHIP-TREND-0 have been supported by a joint grant from Siemens Healthineers, Erlangen, Germany and the Federal State of Mecklenburg-West Pomerania. This study was carried out in collaboration with the German Centre for Cardiovascular Research (DZHK), which is supported by the German Federal Ministry of Education and Research (BMBF).

### **Conflicts of interest**

SEP provides consultancy to and owns stock of Cardiovascular Imaging Inc, Calgary, Alberta, Canada.

## References

1. Aronow WS. Hypertension and left ventricular hypertrophy. *Annals of Translational Medicine*. 2017;5(15):310.
2. Gottdiener JS. The Shape of LVH in Hypertension. *JACC: Cardiovascular Imaging*. 2015;8(9):1042–1044.
3. Mancia G, Rosei EA, Azizi M, Burnier M, Clement DL, Coca A, de Simone G, Dominiczak A, Kahan T, Mahfoud F, et al. 2018 ESC/ESH Guidelines for the management of arterial hypertension. :98.
4. Mancia G, Kreutz R, Brunström M, Burnier M, Grassi G, Januszewucs A, Muiesan ML, Tsioufis K, Agabiti-Reei E, Elhady Algharably EA, et al. 2023 ESH Guidelines for the management of arterial hypertension The Task Force for the management of arterial hypertension of the European Society of Hypertension: Endorsed by the International Society of Hypertension (ISH) and the European Renal Association (ERA). *Journal of Hypertension*. 2023;41(12):1874-2071.
5. Rodrigues JCL, Amadu AM, Dastidar AG, Szantho GV, Lyen SM, Godsave C, Ratcliffe LEK, Burchell AE, Hart EC, Hamilton MCK, et al. Comprehensive characterisation of hypertensive heart disease left ventricular phenotypes. *Heart*. 2016;102(20):1671–1679.
6. Ha ET, Ivanov A, Yeoboah J, Seals A, Peterson SJ, Parikh M, Aronow WS, Frishman WH. Left ventricular hypertrophy subtype and long-term mortality in those with subclinical cardiovascular disease: The Multi-Ethnic Study of Atherosclerosis (MESA). *medRxiv*. 2022:2022.01.29.22270084.
7. Krumholz HM, Larson M, Levy D. Prognosis of left ventricular geometric patterns in the Framingham heart study. *Journal of the American College of Cardiology*. 1995;25(4):879–884.
8. Schillaci G, Verdecchia P, Borgioni C, Ciucci A, Guerrieri M, Zampi I, Battistelli M, Bartoccini C, Porcellati C. Improved electrocardiographic diagnosis of left ventricular hypertrophy. *The American journal of cardiology*. 1994;74(7).
9. Bacharova L, Estes Jr EH, Hill JA, Pahlm I, Schillaci G, Strauss D, Wagner G. Changing role of ECG in the evaluation left ventricular hypertrophy. *Journal of Electrocardiology*. 2012;45(6):609–611.

10. Schillaci G, Battista F, Pucci G. A review of the role of electrocardiography in the diagnosis of left ventricular hypertrophy in hypertension. *Journal of Electrocardiology*. 2012;45(6):617–623.
11. Whelton PK, Carey RM, Aronow WS, Donald E, Casey J, Collins KJ, Himmelfarb CD, DePalma SM, Gidding S, Jamerson KA, Jones DW, et al. 2017 ACC/AHA/AAPA/ABC/ACPM/AGS/APhA/ASH/ASPC/NMA/PCNA Guideline for the Prevention, Detection, Evaluation, and Management of High Blood Pressure in Adults: A Report of the American College of Cardiology/American Heart Association Task Force on Clinical Practice Guidelines. *Hypertension*. 2018.
12. Minardi J, D'Angelo J, Davis S, Davidov D. 100 Are Emergency Physicians Good Enough at Detecting Left Ventricular Hypertrophy on Electrocardiogram? *Annals of Emergency Medicine*. 2012;60(4):S37.
13. Sahota G, Taggar JS. Interpretation of electrocardiograms in primary care. *The British journal of general practice : the journal of the Royal College of General Practitioners*. 2016;66(649).
14. Begg G, Willan K, Tyndall K, Pepper C, Tayebjee M. Electrocardiogram interpretation and arrhythmia management: a primary and secondary care survey. *The British journal of general practice : the journal of the Royal College of General Practitioners*. 2016;66(646).
15. Petersen SE, Matthews PM, Bamberg F, Bluemke DA, Francis JM, Friedrich MG, Leeson P, Nagel E, Plein S, Rademakers FE, et al. Imaging in population science: cardiovascular magnetic resonance in 100,000 participants of UK Biobank - rationale, challenges and approaches. *Journal of Cardiovascular Magnetic Resonance: Official Journal of the Society for Cardiovascular Magnetic Resonance*. 2013;15:46.
16. Petersen SE, Matthews PM, Francis JM, Robson MD, Zemrak F, Boubertakh R, Young AA, Hudson S, Weale P, Garratt S, et al. UK Biobank's cardiovascular magnetic resonance protocol. *Journal of Cardiovascular Magnetic Resonance: Official Journal of the Society for Cardiovascular Magnetic Resonance*. 2016;18:8.
17. Tobin M, Sheehan NA, Scurrah KJ, Burton PR. Adjusting for treatment effects in studies of quantitative traits: antihypertensive therapy and systolic blood pressure. *Statistics in medicine*. 2005;24(19).

18. de Marvao A, McGurk KA, Zheng SL, Thanaj M, Bai W, Duan J, Biffi C, Mazzarotto F, Statton B, Dawes TJW, et al. Phenotypic Expression and Outcomes in Individuals With Rare Genetic Variants of Hypertrophic Cardiomyopathy. *Journal of the American College of Cardiology*. 2021.
19. Mosteller RD. Simplified calculation of body-surface area. *The New England journal of medicine*. 1987;317(17).
20. MATLAB version: 9.13.0 (R2021a), Natick, Massachusetts: The MathWorks Inc. 2021.
21. Naderi H, Ramírez J, van Duijvenboden S, Pujadas ER, Aung N, Wang L, Anwar Ahmed Chahal C, Lekadir K, Petersen SE, Munroe PB. Predicting left ventricular hypertrophy from the 12-lead electrocardiogram in the UK Biobank imaging study using machine learning. *European Heart Journal - Digital Health*. 2023;4:316-324.
22. Nissen SE, Tuzcu EM, Schoenhagen P, Crowe T, Sasiela WJ, Tsai J, Orazem J, Magorien RD, O'Shaughnessy C, Ganz P. Statin Therapy, LDL Cholesterol, C-Reactive Protein, and Coronary Artery Disease. <https://doi.org/10.1056/NEJMoa042000>. 2005.
23. Fit multiclass models for support vector machines or other classifiers - MATLAB fitcecoc - The MathWorks Inc. 2021..
24. Fit ensemble of learners for classification - MATLAB fitcensemble - The MathWorks Inc. 2021..
25. Völzke H. Study of Health in Pomerania (SHIP). *Bundesgesundheitsblatt - Gesundheitsforschung - Gesundheitsschutz*. 2012;55(6):790–794.
26. Völzke H, Schössow J, Schmidt CO, Jürgens C, Richter A, Werner A, Werner N, Radke D, Teumer A, Ittermann T, et al. Cohort Profile Update: The Study of Health in Pomerania (SHIP). *International Journal of Epidemiology*. 2022;51(6):e372–e383.
27. Bycroft C, Freeman C, Petkova D, Band G, Elliott LT, Sharp K, Motyer A, Vukcevic D, Delaneau O, O'Connell J, Cortes A, Welsh S, Young A, Effingham M, McVean G, et al. The UK Biobank resource with deep phenotyping and genomic data. *Nature*. 2018;562(7726):203–209.
28. RStudio Team (2020). RStudio: Integrated Development for R. RStudio, PBC, Boston, MA  
URL <http://www.rstudio.com/>.
29. Kuhn M. building predictive models in R using the caret package. *Journal of Statistical Software*. 2008, 28(5), 1-26.

30. Buuren S van, Groothuis-Oudshoorn K. mice: Multivariate Imputation by Chained Equations in R. *Journal of Statistical Software*. 2011;45:1–67.
31. Bacharova L. Electrical and Structural Remodeling in Left Ventricular Hypertrophy—A Substrate for a Decrease in QRS Voltage? *Annals of Noninvasive Electrocardiology*. 2007;12(3):260–273.
32. Levy D, Labib SB, Anderson KM, Christiansen JC, Kannel WB, Castelli WP. Determinants of sensitivity and specificity of electrocardiographic criteria for left ventricular hypertrophy. *Circulation*. 1990.
33. Beneyto M, Ghyaza G, Cariou E, Amar J, Lairez O. Development and validation of machine learning algorithms to predict left ventricular hypertrophy etiology. *Archives of Cardiovascular Diseases Supplements*. 2023;15(1):109.
34. Slivnick J, Lampert BC. Hypertension and Heart Failure. *Heart Failure Clinics*. 2019;15(4):531–541.
35. Messerli FH, Rimoldi SF, Bangalore S. The Transition From Hypertension to Heart Failure: Contemporary Update. *JACC: Heart Failure*. 2017;5(8):543–551.
36. Nauta JF, Hummel YM, Tromp J, Ouwerkerk W, Meer P van der, Jin X, Lam CSP, Bax JJ, Metra M, Samani NJ, et al. Concentric vs. eccentric remodelling in heart failure with reduced ejection fraction: clinical characteristics, pathophysiology and response to treatment. *European Journal of Heart Failure*. 2020;22(7):1147.
37. Fuchs FD, Whelton PK. High Blood Pressure and Cardiovascular Disease. *Hypertension*. 2020.
38. Lee V, Zheng Q, Toh D-F, Pua CJ, Bryant JA, Lee C-H, Cook SA, Butler J, Díez J, Richards AM, et al. Sacubitril/valsartan versus valsartan in regressing myocardial fibrosis in hypertension: a prospective, randomized, open-label, blinded endpoint clinical trial protocol. *Frontiers in Cardiovascular Medicine*. 2023;10:1248468.
39. National Institute for Health and Care Excellence Guidance. Hypertension in adults: diagnosis and management. 2019. <https://www.nice.org.uk/guidance/ng136>
40. Chen T, Guestrin C. XGBoost: A Scalable Tree Boosting System. *arXiv.org*. 2016.
41. Blockeel H, Devos L, Frénay B, Nanfack G, Nijssen S. Decision trees: from efficient prediction to responsible AI. *Frontiers in Artificial Intelligence*. 2023;6.

42. Cunningham P, Delany SJ. k-Nearest Neighbour Classifiers: 2nd Edition (with Python examples). *arXiv.org*. 2020.

## Tables

**Table 1. Baseline characteristics of UK Biobank participants.**

	<b>Overall (N=20,439)</b>	<b>Normal LV (N= 19,408)</b>	<b>LV remodeling (N=758)</b>	<b>Eccentric LVH (N=181)</b>	<b>Concentric LVH (N= 92)</b>	<b>P-value</b>
Age (years)	66 [11]	66 [11]	68 [10]	63 [13]	67 [9]	<b>0.008</b>
Sex (%)						<b>&lt;0.001</b>
Female	9,335 (45.7)	8,744 (45.1)	457 (60.3)	77 (42.5)	57 (62.0)	
BMI (kg/m <sup>2</sup> )	26.7 [5.2]	26.6 [2.8]	28.5 [5.8]	25.9 [5.0]	27.3 [6.5]	<b>&lt;0.001</b>
Systolic BP (mmHg)	149 [24]	148 [23]	156 [26]	158 [27]	159 [30]	<b>&lt;0.001</b>
Diastolic BP (mmHg)	85 [14]	85 [14]	88 [15]	86 [16]	90 [17]	<b>&lt;0.001</b>
High cholesterol (%)	14,475 (70.8)	13,711 (70.6)	576 (76.0)	118 (65.2)	14,475 (76.1)	<b>0.03</b>
Total cholesterol (mmol/L)	5.0 [1.4]	5.0 [1.4]	5.0 [1.3]	5.0 [1.3]	5.0 [1.4]	0.9
Non-HDL cholesterol (mmol/L)	3.5 [1.3]	3.5 [1.3]	3.5 [1.2]	3.5 [1.3]	3.4 [1.3]	0.7
Diabetes (%)	1,422 (7.0)	1,277 (6.6)	121 (16.0)	12 (6.6)	12 (13.0)	<b>&lt;0.001</b>
Smoking status (%)						<b>&lt;0.001</b>
Never	12,059 (59.0)	11,518 (59.3)	392 (51.7)	99 (54.7)	50 (54.3)	
Previous	7,157 (35.0)	6,770 (34.9)	288 (38.0)	65 (35.9)	34 (37.0)	
Current	1,223 (6.0)	1,120 (5.8)	78 (10.3)	17 (9.4)	8 (8.7)	
Alcohol intake (%)						0.2
Never	908 (4.4)	852 (4.4)	46 (6.1)	7 (3.9)	<5 (3.3)	
Current	19,531 (95.6)	18,556 (95.6)	712 (93.9)	174 (96.1)	89 (96.7)	
Global ECG indices						
Ventricular rate (beats/min)	63 [13]	62 [13]	70 [16]	56 [13]	63 [12]	<b>&lt;0.001</b>
Sokolow-Lyon (%)	403 (2.0)	360 (1.9)	26 (3.4)	11 (6.1)	6 (6.5)	<b>&lt;0.001</b>
Cornell voltage (%)	1,663 (8.1)	1,573 (8.1)	67 (8.8)	12 (6.6)	11 (12.0)	0.4
Pathological Q waves (%)	301 (1.5)	342 (1.8)	17 (2.2)	15 (8.3)	6 (6.5)	<b>&lt;0.001</b>
ST segment deviation (mV)	0.01 [0.03]	0.01 [0.03]	0.02 [0.03]	0.01 [0.03]	0.01 [0.03]	0.8
QT dispersion (ms)	58 [48]	58 [47]	61 [58]	75 [44]	65 [56]	<b>&lt;0.001</b>
Corrected QT duration (ms)	385 [31]	385 [31]	394 [28]	389 [36]	389 [30]	<b>&lt;0.001</b>

P wave amplitude (mV)	0.05 [0.05]	0.05 [0.05]	0.04 [0.04]	0.06 [0.06]	0.05 [0.04]	<b>&lt;0.001</b>
P wave terminal force in V1 (mV/ms)	-2.1[2.8]	-2.1[2.8]	-2.5 [2.9]	-1.7 [3.0]	-2.5 [3.5]	0.08
P wave duration (ms)	112 [22]	112 [22]	108 [20]	110 [28]	112 [15]	<b>0.01</b>
Q wave amplitude (mV)	-0.08 [0.3]	-0.08 [0.04]	-0.08 [0.05]	-0.09 [0.05]	-0.08 [0.05]	<b>0.02</b>
Q wave duration (ms)	23 [4]	23 [4]	23 [5]	25 [5]	24 [6]	<b>&lt;0.001</b>
R wave amplitude (mV)	0.49 [0.23]	0.49 [0.23]	0.48 [0.22]	0.55 [0.31]	0.58 [0.31]	<b>&lt;0.001</b>
S wave amplitude (mV)	-0.30 [0.19]	-0.30 [0.18]	-0.32 [0.21]	-0.42 [0.26]	-0.38 [0.26]	<b>&lt;0.001</b>
QRS amplitude (mV)	0.92 [0.30]	0.92 [0.30]	0.92 [0.30]	1.15 [0.37]	1.14 [0.37]	<b>&lt;0.001</b>
QRS duration (ms)	90 [16]	90 [16]	90 [18]	97 [16]	98 [15]	<b>&lt;0.001</b>
QRS ascending slope (mV/s)	34.5 [15.1]	34.5 [15.4]	34.8 [15.3]	36.1 [18.3]	39.7 [17]	<b>&lt;0.001</b>
QRS descending slope (mV/s)	-53.9 [-18.9]	-53.7 [18.5]	-55.5 [18.7]	-64.9 [22.0]	-66.6 [24.7]	<b>&lt;0.001</b>
T wave amplitude (mV)	0.14 [0.07]	0.14 [0.07]	0.13 [0.06]	0.15 [0.08]	0.14 [0.08]	<b>&lt;0.001</b>
T wave duration (ms)	108 [16]	108 [16]	108 [16]	110 [18]	109 [19]	<b>&lt;0.001</b>

**Legend.** Counts variables are presented as number (percentage), continuous variables as median [interquartile range]. To assess for associations between participants with LVH-mediated LVH phenotypes, the Wilcoxon signed-rank test was used for continuous data and Fisher's exact test for categorical data. Global ECG indices are the median values calculated from the independent leads of the 12-lead ECG. Blood pressure and cholesterol values are adjusted for medication use. BMI: body mass index, BP: blood pressure, LV: left ventricle, LVH: left ventricular hypertrophy, mmHg: millimetres mercury, mmol/L: millimoles per litre, ms: milliseconds, mV: millivolts, s: seconds.

**Table 2. Baseline characteristics of participants in the Study of Health in Pomerania.**

	<b>Overall (N=877)</b>	<b>Normal LV (N= 704)</b>	<b>LV remodeling (N=134)</b>	<b>Eccentric LVH (N=12)</b>	<b>Concentric LVH (N= 27)</b>	<b>P-value</b>
Age (years)	56 [19]	55 [20]	61 [16]	49 [27]	59 [15]	<b>0.02</b>
Sex (%)						<b>0.04</b>
Female	344 (39.2)	261 (37.1)	67 (50.0)	6 (50.0)	10 (37.0)	
BMI (kg/m <sup>2</sup> )	28.0 [5.4]	27.7 [5.4]	29.5 [5.1]	25.1 [4.3]	30.0 [5.8]	<b>0.007</b>
Systolic BP (mmHg)	135 [18]	135 [18]	135 [22]	132 [22]	145 [20]	<b>&lt;0.001</b>
Diastolic BP (mmHg)	82 [13]	82 [12]	81 [15]	75 [17]	83 [12]	0.3
High cholesterol (%)	693 (79.0)	542 (77.0)	121 (90.3)	8 (66.7)	22 (81.5)	<b>0.004</b>
Total cholesterol (mmol/L)	5.8 [1.4]	5.8 [1.3]	6.1 [1.4]	5.4 [1.6]	6.0 [1.5]	<b>0.01</b>
Non-HDL cholesterol (mmol/L)	4.4 [1.3]	4.3 [1.4]	4.6 [1.2]	4.0 [2.1]	4.7 [1.3]	<b>0.01</b>
Diabetes (%)	772 (88.0)	618 (87.8)	120 (89.6)	9 (75.0)	25 (92.6)	0.4
Smoking status (%)						<b>0.008</b>
Previous	728 (83.0)	597 (84.8)	105 (78.4)	9 (75.0)	17 (63.0)	
Current	149 (17.0)	107 (15.2)	29 (21.6)	<5 (25.0)	10 (37.0)	
Alcohol intake (%)						0.2
Never	53 (6.0)	41 (5.8)	10 (7.5)	<5 (16.7)	0 (0)	
Current	824 (94.0)	663 (94.2)	124 (92.5)	10 (83.3)	27 (100.0)	
<b>Global ECG indices</b>						
Ventricular rate (beats/min)	64 [14]	63 [14]	68 [13]	62 [10]	65 [16]	<b>0.04</b>
Sokolow-Lyon (%)	50 (5.7)	37 (5.3)	6 (4.5)	<5 (25.0)	<5 (14.8)	<b>0.004</b>
Cornell voltage (%)	75 (8.6)	62 (8.8)	10 (7.5)	<5 (8.3)	<5 (7.4)	0.9
ST segment deviation (mV)	0.03 [0.03]	0.03 [0.03]	0.03 [0.03]	0.03 [0.05]	0.03 [0.03]	0.7
QT dispersion (ms)	47 [45]	44 [45]	45 [51]	72 [22]	60 [39]	<b>0.04</b>
Corrected QT duration (ms)	384 [27]	384 [29]	387 [26]	378 [36]	387 [26]	0.2
P wave amplitude (mV)	0.02 [0.03]	0.02 [0.03]	0.02 [0.03]	0.01 [0.03]	0.03 [0.01]	0.7
P wave terminal force in V1 (mV/ms)	-2.8 [2.3]	-2.8 [2.3]	-3.2 [2.2]	-1.8 [1.6]	-2.5 [2.1]	0.5

P wave duration (ms)	86 [20]	86 [18]	86 [20]	79 [12]	86 [23]	0.8
Q wave amplitude (mV)	-0.10 [0.05]	-0.10 [0.05]	-0.09 [0.04]	-0.10 [0.06]	-0.12 [0.05]	0.3
Q wave duration (ms)	24 [4]	24 [4]	24 [4]	24 [3]	23 [4]	0.3
R wave amplitude (mV)	0.55 [0.24]	0.55 [0.23]	0.53 [0.26]	0.65 [0.18]	0.63 [0.38]	0.4
S wave amplitude (mV)	-0.24 [0.16]	-0.23 [0.16]	-0.25 [0.18]	-0.24 [0.13]	-0.28 [0.18]	0.1
QRS amplitude (mV)	0.98 [0.35]	0.98 [0.33]	0.96 [0.34]	1.22 [0.27]	1.20 [0.40]	0.7
QRS duration (ms)	90 [10]	90 [10]	89 [9]	90 [10]	92 [9]	0.1
QRS ascending slope (mV/s)	37.9 [14.9]	37.6 [14.3]	38.1 [17.3]	41.1 [9.0]	44.0 [25.9]	0.4
QRS descending slope (mV/s)	-55.1 [19.6]	-54.7 [18.8]	-54.8 [21.5]	-67.1 [21.9]	-62.0 [26.6]	0.1
T wave amplitude (mV)	0.16 [0.08]	0.16 [0.08]	0.15 [0.07]	0.16 [0.13]	0.14 [0.08]	0.6
T wave duration (ms)	112 [18]	112 [18]	108 [16]	120 [12]	110 [21]	0.4

**Legend.** Counts variables are presented as number (percentage), continuous variables as median [interquartile range]. To assess for associations between participants with LVH-mediated LVH phenotypes, the Wilcoxon signed-rank test was used for continuous data and Fisher's exact test for categorical data. Global ECG indices are the median values calculated from the independent leads of the 12-lead ECG. Blood pressure and cholesterol values are adjusted for medication use. BMI: body mass index, BP: blood pressure, LV: left ventricle, LVH: left ventricular hypertrophy, mmHg: millimetres mercury, mmol/L: millimoles per litre, ms: milliseconds, mV: millivolts, s: seconds.

**Table 3. Performance metrics of supervised machine learning classifiers using ECG and clinical variables in UK Biobank and validation testing in Study of Health in Pomerania.**

	UK Biobank			Validation in SHIP
	Logistic regression	Support vector machine	Random forest	Support vector machine
Accuracy (%)	0.74	0.79	0.73	0.75
Sensitivity (%)	0.47	0.59	0.45	0.51
Specificity (%)	0.83	0.87	0.82	0.85
Precision (%)	0.68	0.78	0.64	0.63
F1 score (%)	0.56	0.67	0.53	0.56
AUC	0.71	0.69	0.70	0.65

*AUC: area under the receiver operator curve; LVH: left ventricular hypertrophy; SHIP: Study of Health in Pomerania.*



**Figure 1. Flow diagram illustrating the steps involved in UK Biobank participant selection.**

*CMR: cardiac magnetic resonance imaging; HCM: hypertrophic cardiomyopathy; LV: left ventricle; LVH: left ventricular hypertrophy.*

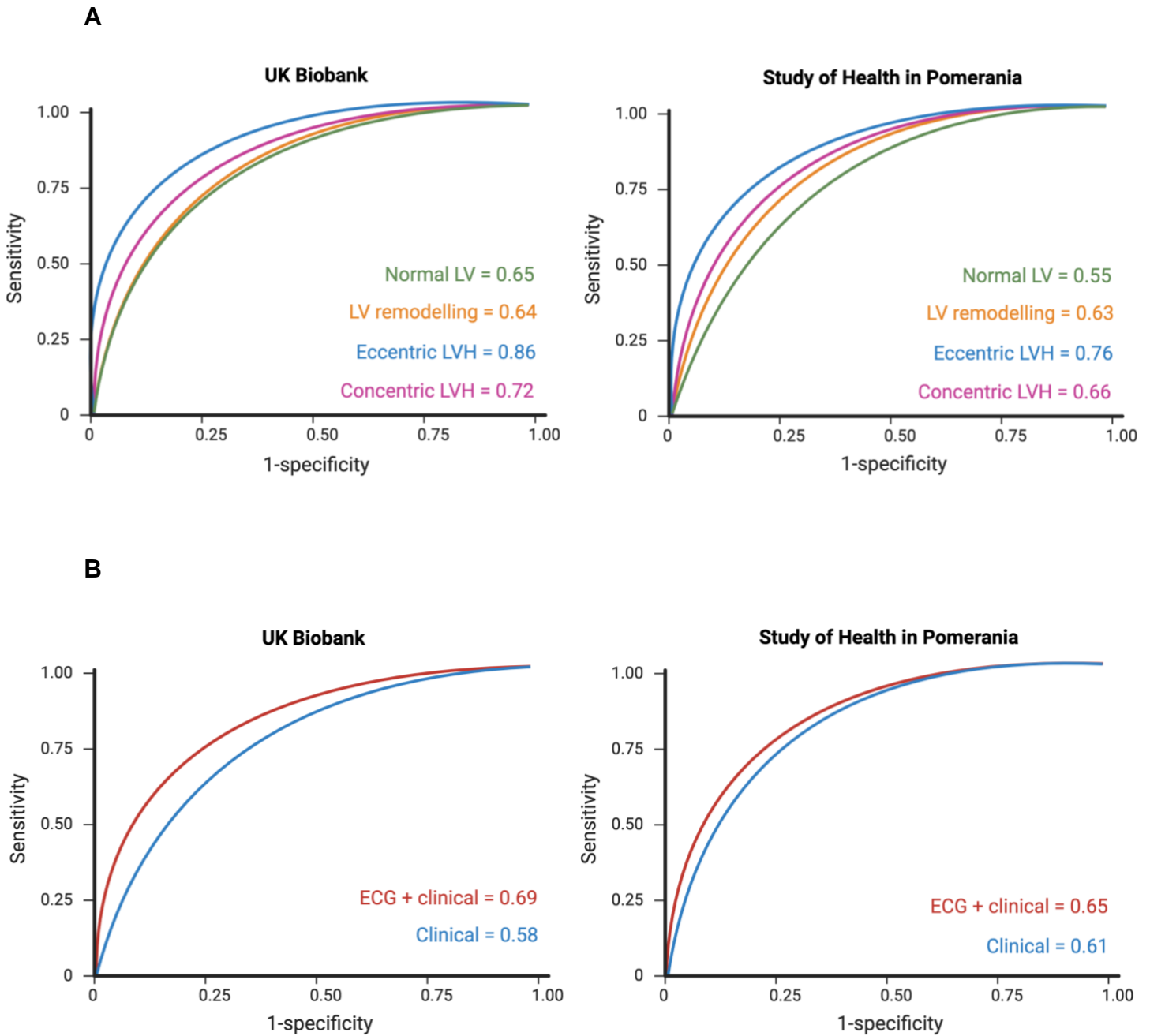


**Figure 2. (A) Classification of hypertension mediated LVH phenotypes in UK Biobank and Study of Health in Pomerania using support vector machine.**

**(B) Classification of hypertension mediated LVH phenotypes using ECG and clinical vs clinical data alone in UK Biobank and Study of Health in Pomerania with support vector machine.**

*ECG: electrocardiogram; LV: left ventricle; LVH: left ventricular hypertrophy.*

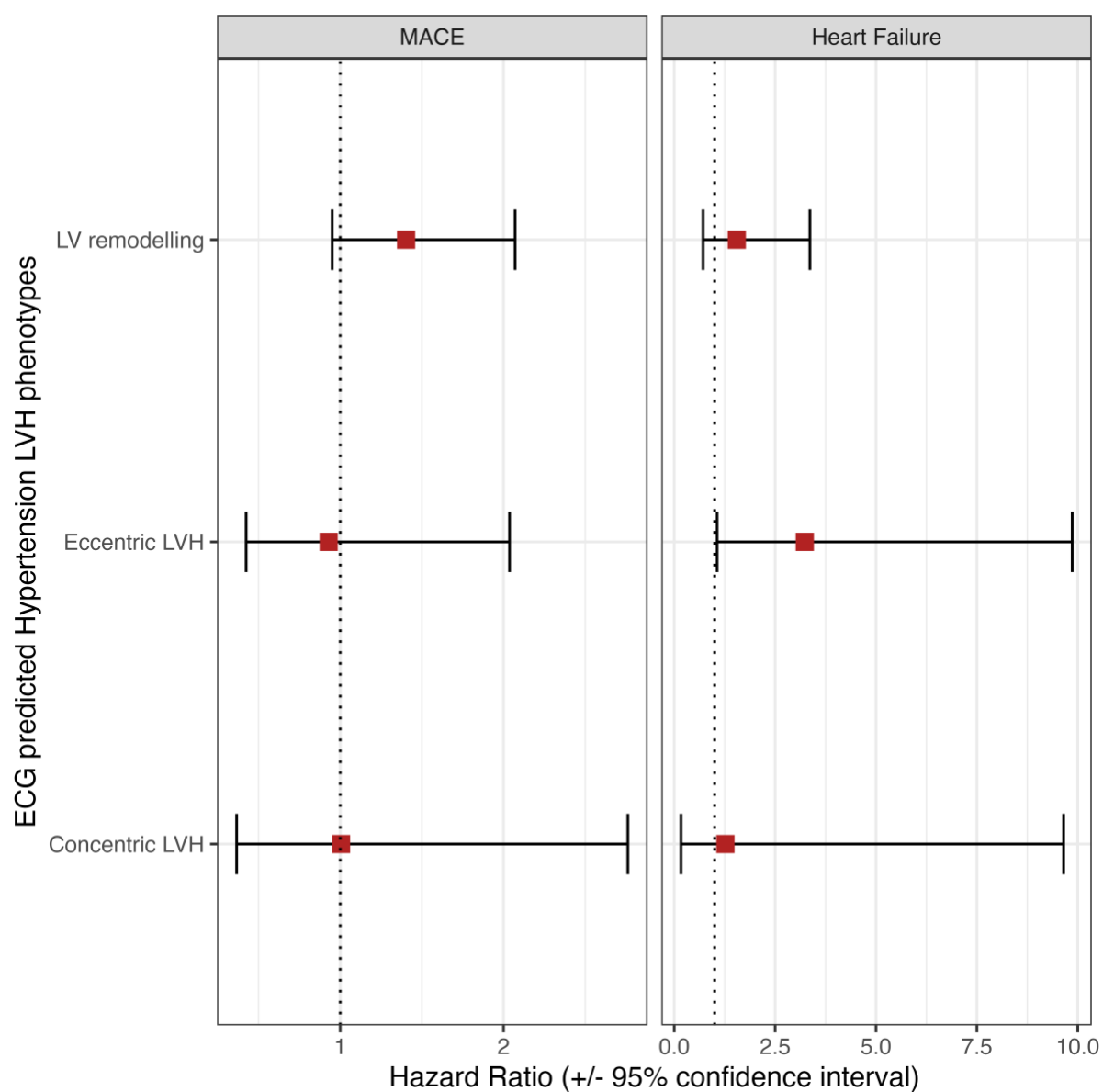


**Figure 3. Associations of ECG-predicted hypertension-mediated LVH phenotypes and clinical outcomes.**

*Results are hazard ratios from Cox hazards proportional regression models. The diseases listed are set as the model outcome (response variable) and hypertension-mediated LV phenotype in the exposure of interest with normal LV as the reference group. The model was adjusted for age, sex and BMI.*

*CI: confidence interval; HR: hazard ratio; MACE: major adverse cardiovascular events; LVH: left ventricular hypertrophy*

## Supplementary material

**Supplementary Table 1.** UK Biobank data fields used to identify hypertensive participants.

Phenotype	Data fields	Field names	Data code definitions
Hypertension	20002	Non-cancer illness code, self-reported	Hypertension, Essential hypertension
Hypertension	6150	Vascular/heart problems diagnosed by doctor	High blood pressure
Hypertension	6177	Medication for cholesterol, blood pressure or diabetes	Blood pressure medication
Hypertension	6153	Medication for cholesterol, blood pressure, diabetes or take exogenous hormones	Blood pressure medication
Hypertension	4080	Systolic blood pressure, automated reading	$\geq 130$ mmHg
Hypertension	4079	Diastolic blood pressure, automated reading	$\geq 85$ mmHg
Hypertension	93	Systolic blood pressure, manual reading	$\geq 130$ mmHg
Hypertension	94	Diastolic blood pressure, manual reading	$\geq 85$ mmHg
Aortic stenosis	20002	Non-cancer illness code, self-reported	Aortic stenosis
Hypertrophic cardiomyopathy	20002	Non-cancer illness code, self-reported	Hypertrophic cardiomyopathy

**Supplementary Table 2.** Definition of ECG biomarkers associated with LVH.

ECG marker	Definition
Sokolow-Lyon index	$(SV1 \text{ or } SV2) + (RV5 \text{ or } RV6) > 35\text{mm}$ or R wave in aVL $\geq 11\text{mm}$
Cornell voltage	$SV3 + RaVL > 28\text{mm}$ (men) $> 20\text{mm}$ (women)
Pathological Q waves	$> 30\text{ms}$ in duration and $> 1/3$ of the R wave in depth in two or more contiguous leads (I, II, V1-6)
R wave amplitude (mV)	Amplitude of R wave in V5 or V6 $> 2.6\text{mV}$ , in aVL $> 1.1\text{mV}$
QRS amplitude (mV)	Absolute value of the difference between maximum and minimum of the QRS complex values
QRS duration (ms)	QRS width from beginning of Q wave to end of S wave, ( $\geq 90\text{ms}$ )
QRS ascending slope	Upward slope of QRS complex
QRS descending slope	Downward slope of QRS complex
QTc interval (ms)	Prolonged corrected QT $\geq 450\text{ms}$ (men) $\geq 460\text{ms}$ (women)
STT segment amplitude	Absolute value of the difference between maximum and minimum of the ST segment values
ST segment displacement	Difference between the beginning of the QRS complex and the beginning of the T wave
QTc dispersion	Inter lead variations in QT segment length ( $< 40\text{ms}$ )
T wave inversion	T wave amplitude $\leq -0.1\text{mV}$ or a negative inflexion of at least $0.1\text{mV}$ in lead I, II or V3-6
T wave amplitude (mV)	Absolute value of the difference between maximum and minimum of the T wave complex values
T wave axis ( $^{\circ}$ )	$< -15^{\circ}$ to $\geq -180^{\circ}$ or $> 105^{\circ}$ to $\leq 180^{\circ}$
T peak to T end interval (ms)	Duration between the peak of the T wave and the end of the T wave in each lead

**Supplementary Table 3.** Codes used to define clinical outcomes using ICD-9, ICD-10 and OPCS4 codes.

<b>Myocardial Infarction</b>	
<b>ICD10 codes</b>	<b>Definition</b>
I21	Acute myocardial infarction
I21.0	Acute transmural myocardial infarction of anterior wall
I21.1	Acute transmural myocardial infarction of inferior wall
I21.2	Acute transmural myocardial infarction of other sites
I21.3	Acute transmural myocardial infarction of unspecified site
I21.4	Acute subendocardial myocardial infarction
I21.9	Acute myocardial infarction, unspecified
I22	Subsequent myocardial infarction
I22.0	Subsequent myocardial infarction of anterior wall
I22.1	Subsequent myocardial infarction of inferior wall
I22.8	Subsequent myocardial infarction of other sites
I22.9	Subsequent myocardial infarction of unspecified site
I23	Certain current complications following acute myocardial infarction
I23.0	Haemopericardium as current complication following acute myocardial infarction
I23.1	Atrial septal defect as current complication following acute myocardial infarction
I23.2	Ventricular septal defect as current complication following acute myocardial infarction
I23.3	Rupture of cardiac wall without haemopericardium as current complication following acute myocardial infarction
I23.5	Rupture of papillary muscle as current complication following acute myocardial infarction
I23.6	Thrombosis of atrium, auricular appendage and ventricle as current complications following acute myocardial infarction
I23.8	Other current complications following acute myocardial infarction
I24	Other acute ischaemic heart disease
I24.0	Coronary thrombosis not resulting in myocardial infarction
I24.1	Dressler's syndrome
I24.8	Other forms of acute ischaemic heart disease
I24.9	Acute ischaemic heart disease, unspecified
I25	Chronic ischaemic heart disease
I25.0	Atherosclerotic cardiovascular disease
I25.1	Atherosclerotic heart disease
I25.2	Old myocardial infarction
I25.3	Aneurysm of heart
I25.4	Coronary artery aneurysm
I25.5	Ischaemic cardiomyopathy
I25.6	Silent myocardial ischaemia
I25.8	Other forms of chronic ischaemic heart disease
I25.9	Chronic ischaemic heart disease, unspecified
<b>ICD9 codes</b>	<b>Definition</b>

4109	Acute myocardial infarction
<b>OPCS4</b>	<b>Definition</b>
K40	Saphenous vein graft replacement of coronary artery
K40.1	Saphenous vein graft replacement of one coronary artery
K40.2	Saphenous vein graft replacement of two coronary arteries
K40.3	Saphenous vein graft replacement of three coronary arteries
K40.4	Saphenous vein graft replacement of four or more coronary arteries
K40.8	Other specified saphenous vein graft replacement of coronary artery
K40.9	Unspecified saphenous vein graft replacement of coronary artery
K41	Other autograft replacement of coronary artery
K41.1	Autograft replacement of one coronary artery NEC
K41.2	Autograft replacement of two coronary arteries NEC
K41.3	Autograft replacement of three coronary arteries NEC
K41.4	Autograft replacement of four or more coronary arteries NEC
K41.8	Other specified other autograft replacement of coronary artery
K41.9	Unspecified other autograft replacement of coronary artery
K42	Allograft replacement of coronary artery
K42.1	Allograft replacement of one coronary artery
K42.2	Allograft replacement of two coronary arteries
K42.3	Allograft replacement of three coronary arteries
K42.4	Allograft replacement of four or more coronary arteries
K42.8	Other specified other allograft replacement of coronary artery
K42.9	Unspecified other allograft replacement of coronary artery
K44	Other replacement of coronary artery
K44.1	Replacement of coronary arteries using multiple methods
K44.2	Revision of replacement of coronary artery
K44.8	Other specified other replacement of coronary artery
K44.9	Unspecified other replacement of coronary artery
K45	Connection of thoracic artery to coronary artery
K45.1	Double anastomosis of mammary arteries to coronary arteries
K45.2	Double anastomosis of thoracic arteries to coronary arteries NEC
K45.3	Anastomosis of mammary artery to left anterior descending coronary artery
K45.4	Anastomosis of mammary artery to coronary artery NEC
K45.5	Anastomosis of thoracic artery to coronary artery NEC
K45.6	Revision of connection of thoracic artery to coronary artery
K45.8	Other specified connection of thoracic artery to coronary artery
K45.9	Unspecified connection of thoracic artery to coronary artery
K49	Transluminal balloon angioplasty of coronary artery
K49.1	Percutaneous transluminal balloon angioplasty of one coronary artery
K49.2	Percutaneous transluminal balloon angioplasty of multiple coronary arteries
K49.3	Percutaneous transluminal balloon angioplasty of bypass graft of coronary artery
K49.4	Percutaneous transluminal cutting balloon angioplasty of coronary artery
K49.8	Other specified transluminal balloon angioplasty of coronary artery
K49.9	Unspecified transluminal balloon angioplasty of coronary artery
K50	Other therapeutic transluminal operations on coronary artery
K50.1	Percutaneous transluminal laser coronary angioplasty
K50.2	Percutaneous transluminal coronary thrombolysis using streptokinase
K50.3	Percutaneous transluminal injection of therapeutic substance into coronary artery NEC
K50.4	Percutaneous transluminal atherectomy of coronary artery
K50.8	Other specified other therapeutic transluminal; operations on coronary artery

K50.9	Unspecified other therapeutic transluminal operations on coronary artery
K75	Percutaneous transluminal balloon angioplasty and insertion of stent into coronary artery
K75.1	Percutaneous transluminal balloon angioplasty and insertion of 1-2 drug-eluting stents into coronary artery
K75.2	Percutaneous transluminal balloon angioplasty and insertion of 3 or more drug-eluting stents into coronary artery
K75.3	Percutaneous transluminal balloon angioplasty and insertion of 1-2 stents into coronary artery
K75.4	Percutaneous transluminal balloon angioplasty and insertion of 3 or more stents into coronary artery NEC
K75.8	Other specified percutaneous transluminal balloon angioplasty and insertion of stent into coronary artery
K75.9	Unspecified percutaneous transluminal balloon angioplasty and insertion of stent into coronary artery
<b>Heart Failure</b>	
<b>ICD10 codes</b>	<b>Definition</b>
I11.0	Hypertensive heart disease with (congestive) heart failure
I13.0	Hypertensive heart and renal disease with (congestive) heart failure
I13.2	Hypertensive heart and renal disease with both (congestive) heart failure and renal failure
I25.5	Ischaemic cardiomyopathy
I50	Heart failure
I50.0	Congestive heart failure
I50.1	Left ventricular failure
I50.9	Heart failure, unspecified
J81	Pulmonary oedema
K76.1	Chronic passive congestion of liver
<b>ICD9 codes</b>	<b>Definition</b>
4280	Congestive heart failure
4281	Left heart failure
4289	Heart failure, unspecified
<b>OPCS4 codes</b>	<b>Definition</b>
K59.6	Implantation of cardioverter defibrillator using three electrode leads
K61.7	Implantation of biventricular cardiac pacemaker system
K60.7	Implantation of intravenous biventricular cardiac pacemaker system
<b>Stroke</b>	
<b>ICD10 codes</b>	<b>Definition</b>
I60	Subarachnoid haemorrhage
I60.0	Subarachnoid haemorrhage from carotid siphon bifurcation
I60.1	Subarachnoid haemorrhage from middle cerebral artery
I60.2	Subarachnoid haemorrhage from anterior communicating artery
I60.3	Subarachnoid haemorrhage from posterior communicating artery
I60.4	Subarachnoid haemorrhage from basilar artery
I60.5	Subarachnoid haemorrhage from vertebral artery
I60.6	Subarachnoid haemorrhage from other intracranial arteries

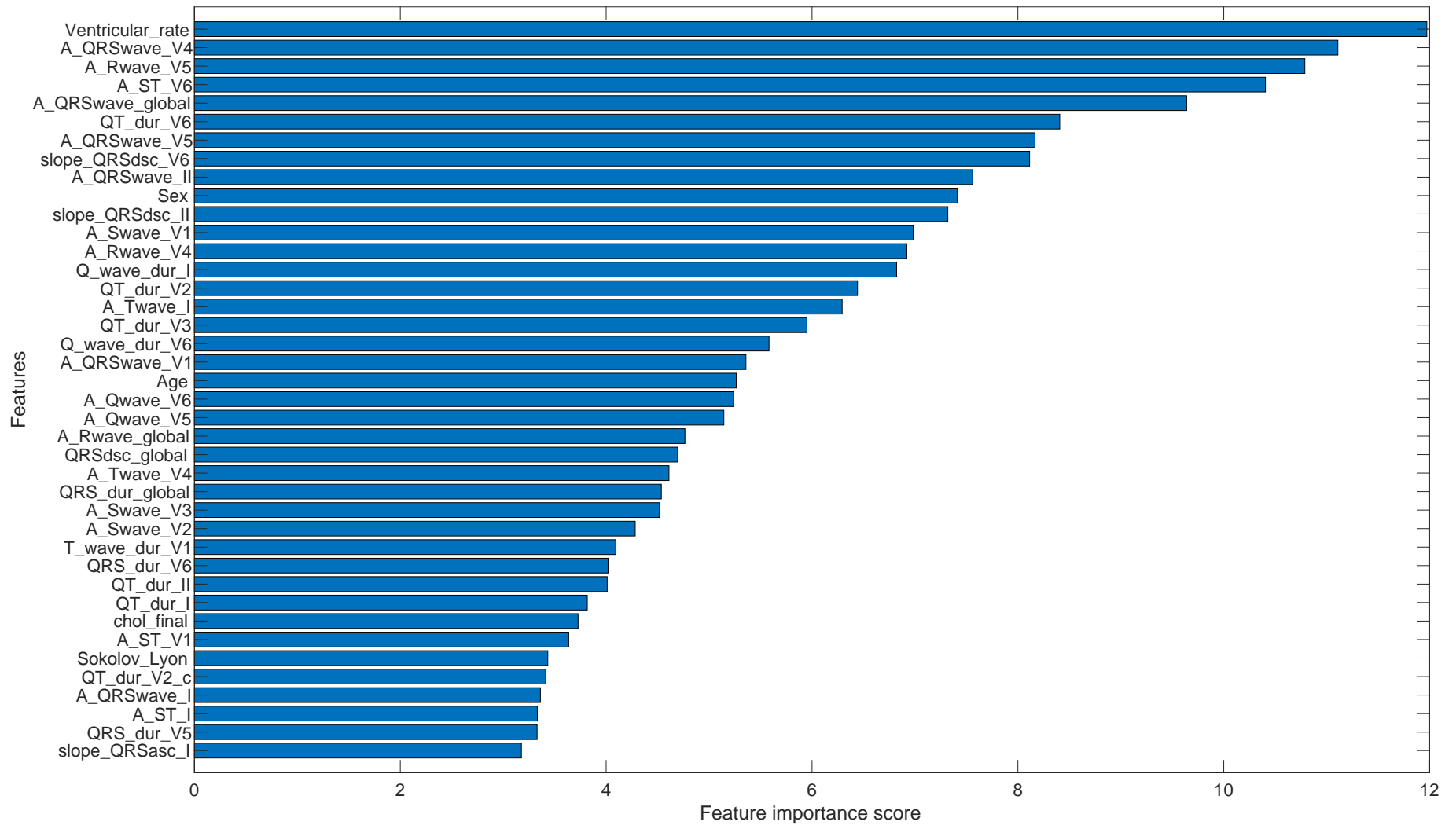
I60.7	Subarachnoid haemorrhage from intracranial artery, unspecified
I60.8	Other subarachnoid haemorrhage
I60.9	Subarachnoid haemorrhage, unspecified
I61	Intracerebral haemorrhage
I61.0	Intracerebral haemorrhage in hemisphere subcortical
I61.1	Intracerebral haemorrhage in hemisphere, cortical
I61.2	Intracerebral haemorrhage in hemisphere, unspecified
I61.3	Intracerebral haemorrhage in brain stem
I61.4	Intracerebral haemorrhage in cerebellum
I61.5	Intracerebral haemorrhage, intraventricular
I61.6	Intracerebral haemorrhage, multiple localised
I61.8	Other intracerebral haemorrhage
I61.9	Intracerebral haemorrhage, unspecified
I62	Other nontraumatic intracranial haemorrhage
I62.0	Subdural haemorrhage (acute) (nontraumatic)
I62.1	Nontraumatic extradural haemorrhage
I62.9	Intracranial haemorrhage (nontraumatic), unspecified
I63	Cerebral infarction
I63.0	Cerebral infarction due to thrombosis of precerebral arteries
I63.1	Cerebral infarction due to embolism of precerebral arteries
I63.2	Cerebral infarction due to unspecified occlusion or stenosis of precerebral arteries
I63.3	Cerebral infarction due to thrombosis of cerebral arteries
I63.4	Cerebral infarction due to embolism of cerebral arteries
I63.5	Cerebral infarction due to unspecified occlusion or stenosis of cerebral arteries
I63.6	Cerebral infarction due to cerebral venous thrombosis, nonpyogenic
I63.8	Other cerebral infarction
I63.9	Cerebral infarction, unspecified
I64	Stroke, not specified as haemorrhage or infarction
I65	Occlusion and stenosis of precerebral arteries, not resulting in cerebral infarction
I65.0	Occlusion and stenosis of vertebral artery
I65.1	Occlusion and stenosis of basilar artery
I65.2	Occlusion and stenosis of carotid artery
I65.3	Occlusion and stenosis of multiple and bilateral precerebral arteries
I65.8	Occlusion and stenosis of other precerebral artery
I65.9	Occlusion and stenosis of unspecified precerebral artery
I66	Occlusion and stenosis of cerebral arteries, not resulting in cerebral infarction
I66.0	Occlusion and stenosis of middle cerebral artery
I66.1	Occlusion and stenosis of anterior cerebral artery
I66.2	Occlusion and stenosis of posterior cerebral artery
I66.3	Occlusion and stenosis of cerebellar arteries
I66.4	Occlusion and stenosis of multiple and bilateral cerebral arteries
I66.8	Occlusion and stenosis of other cerebral artery
I66.9	Occlusion and stenosis of unspecified cerebral artery
I67.0	Dissection of cerebral arteries, nonruptured
I67.8	Other specified cerebrovascular diseases
I67.9	Cerebrovascular disease, unspecified
I69	Sequelae of cerebrovascular disease

<b>ICD9 codes</b>	<b>Definition</b>
4309	Subarachnoid haemorrhage
4319	Intracerebral haemorrhage
4320	Nontraumatic extradural haemorrhage
4321	Subdural haemorrhage
4331	Occlusion and stenosis of carotid artery
4339	Occlusion and stenosis of precerebral arteries, unspecified
4349	Occlusion of cerebral arteries, unspecified
4369	Acute but ill-defined cerebrovascular disease
4371	Other generalised ischaemic cerebrovascular disease
<b>OPCS4 codes</b>	<b>Definition</b>
L35.4	Percutaneous transluminal embolectomy of cerebral artery
<b>Ventricular Arrhythmias</b>	
<b>ICD10 codes</b>	<b>Definition</b>
I47.2	Ventricular tachycardia
I49.0	Ventricular fibrillation and flutter
I46.0	Cardiac arrest with successful resuscitation
I46.1	Sudden cardiac death, so described
I46.9	Cardiac arrest, unspecified
I47.0	Re-entry ventricular arrhythmia
<b>ICD9 codes</b>	<b>Definition</b>
4270	Paroxysmal ventricular tachycardia
4271	Paroxysmal ventricular tachycardia
4272	Paroxysmal tachycardia, unspecified
4274	Ventricular fibrillation and flutter
<b>OPCS4 codes</b>	<b>Definition</b>
K59	Cardioverter defibrillator introduced through vein
K59.1	Implantation of cardioverter defibrillator using one electrode lead
K59.2	Implantation of cardioverter defibrillator using two electrode leads
K59.3	Resitting of leads of cardioverter defibrillator
K59.4	Renewal of cardioverter defibrillator
K59.6	Implantation of cardioverter defibrillator using three electrode leads
K59.8	Other specified cardioverter defibrillator introduced through the vein
K59.9	Unspecified cardioverter defibrillator introduced through the vein
K72	Other cardioverter defibrillator
K72.1	Implantation of subcutaneous cardioverter defibrillator
K72.3	Renewal of subcutaneous cardioverter defibrillator

**Supplementary Table 4. Associations of ECG-predicted hypertension-mediated LVH phenotypes and clinical outcomes.**

	<b>MACE</b>		<b>Heart Failure</b>	
	HR (95% CI)	P-value	HR (95% CI)	P-value
<b>LV remodeling</b>	1.40 (0.37-2.76)	0.1	1.55 (0.71-3.36)	0.3
<b>Eccentric LVH</b>	0.93 (0.42-2.04)	0.9	3.24 (1.06-9.86)	0.04
<b>Concentric LVH</b>	1.01 (0.37-2.76)	0.1	1.27 (0.17-9.65)	0.8

*AUC: area under the receiver operator curve; CI: confidence interval; HR: hazard ratio; MACE: major adverse cardiovascular events; LVH: left ventricular hypertrophy.*



**Supplementary figure 1. Ranking of the top 40 features using chi-squared feature selection.**